47th AIAA Aerospace Sciences Meeting Including The New Horizons Forum and Aerospace Exposition
5 - 8 January 2009, Orlando, Florida

AIAA 2009-685

A Comparison of Smart Rotor Control Approaches using Trailing Edge Flaps and Individual Pitch Control

Matthew A. Lackner* and Gijs van Kuik*

Technical University of Delft, Kluyverweg 1, 2629 HS, Delft, The Netherlands

Modern wind turbines have been steadily increasing in size, and have now become very large, with recent models boasting rotor diameters greater than 120 m. Reducing the loads experienced by the wind turbine rotor blades is one means of lowering the cost of energy of wind turbines. Wind turbines are subjected to significant and rapid fluctuating loads, which arise from a variety of sources including: turbulence in the wind, tower shadow, wind shear, and yawed flow conditions. "Smart rotor control" concepts have emerged as a major topic of research in the attempt to reduce fatigue loads on wind turbines. In this approach, aerodynamic load control devices are distributed along the span of the wind turbine blade, and through a combination of sensing, control, and actuation, these devices dynamically control the loads on the blades. This research investigates the load reduction potential of smart rotor control devices, namely trailing edge flaps (TEFs), in the operation of a 5 MW wind turbine in the aeroelastic design code "GH Bladed." Specifically in this paper, the fatigue load reductions achieved using trailing edge flaps are evaluated, and the performance is compared to another promising load reduction technique, individual pitch control.

A feedback control approach is implemented for load reduction, which utilizes a multi-blade coordinate transformation, so that variables in the rotating frame of reference can be mapped into a fixed frame of reference. Single input single output (SISO) control techniques for linear time invariant (LTI) systems are then employed to determine the appropriate response of the TEFs based on the loads on the blades. The use of TEFs and this control approach is shown to effectively reduce the fatigue loads on the blades, relative to a baseline controller. The load reduction potential is also compared to an alternative individual pitch control approach, in the time and frequency domain. The effects on the pitch and power systems are briefly evaluated, and the limitations of the analysis are assessed.

Nomenclature

C_D	Coefficient of Drag
C_L	Coefficient of Lift
C_M	Coefficient of Pitching Moment
DEL	Damage Equivalent Load
$DTEG$	Deformable Trailing Edge Geometry
FEL	Fatigue Equivalent Load
IFC	Individual Flap Control
IPC	Individual Pitch Control
k	Reduced Frequency
kWh	Kilowatt-Hour
LQR	Linear Quadratic Regulator
LTI	Linear Time Invariant
LTV	Linear Time Varying
M_y	Blade Root Flapwise Bending Moment
PID	Proportional-Integral-Derivative

*Postdoctoral Researcher, Department of Aerospace Engineering, Technical University of Delft, Kluyverweg 1, 2629 HS, Delft, The Netherlands.

SC	Standard Control
$SISO$	Single Input Single Output
TUD	Technical University of Delft
TEF	Trailing Edge Flap
α	Angle of Attack
ϕ	Angle of Relative Wind

I. Introduction

Modern wind turbines have been steadily increasing in size, and have now become very large, with recent models boasting rotor diameters greater than 120 m. As wind turbines increase in size, the primary objective of research and development is to lower the cost of the turbine per kilowatt-hour (kWh) of electricity produced, or "cost of energy." Reducing the loads experienced by the wind turbine rotor blades is one means of lowering the cost of energy. Load reduction on the blades can not only lower the cost of the blades themselves, but can also lead to reduced loads in other components such as the drive train and tower, and therefore lower costs of these components as well.

Wind turbines are subjected to significant and rapid fluctuating loads, which arise from a variety of sources including: turbulence in the wind, tower shadow, wind shear, and yawed flow conditions. As wind turbines becomes larger and more flexible, wind speed variations across the rotor disk become larger, resulting in substantial fluctuating loads, and therefore the importance of load reduction increases.[1] These fluctuating loads, or fatigue loads, can lead to damage of turbine components and eventually to failures. As such, reducing fatigue loads can result in increased component lifetimes, reduced maintenance requirements, and an overall lower cost of energy.

"Smart rotor control" concepts have emerged as a major topic of research in the attempt to reduce fatigue loads on wind turbines. In this approach, aerodynamic load control devices are distributed along the span of the wind turbine blade, and through a combination of sensing, control, and actuation, these devices dynamically control the loads on the blades, at any azimuthal position. Smart rotor control concepts can primarily affect the out-of-plane ("flapwise") blade loads, and while a reduction of fatigue loads is the primary objective, extreme loads may also be mitigated using this approach.

This research investigates the load reduction potential of smart rotor control devices, specifically trailing edge flaps (TEFs), in the operation of a 5 MW wind turbine in the aeroelastic design code "GH Bladed."[2] Several important issues and questions are addressed including:

- Validation of the fatigue load reduction potential of TEFs.
- The relative performance of TEFs compared to other smart rotor control load reduction methods.
- The effect of the smart rotor control approaches on the pitch and power systems.
- The potential limitations of the analysis.

I.A. Previous Work

Smart rotor control has become an active area of research for wind turbine applications.[3] Barlas provides detailed summaries of smart rotor control research for wind turbines, including thorough reviews of potential actuators, sensors, aerodynamic control surfaces, control approaches, and simulation environments.[4]

Individual pitch control (IPC) is a popular potential smart rotor control concept, and several investigations into the use of IPC schemes have been conducted recently. van Engelen and van der Hooft,[5] Bossayni,[6] and Selvam,[7] along with others, have investigated control approaches for IPC, simulated IPC schemes, and demonstrated sizable load reduction capabilities of the IPC approach.

Smart rotor control simulations that utilize localized load control devices have also been conducted. In particular, the work of Andersen et al.,[8] and McCoy and Griffin[9] simulate spanwise distributed load control devices, and provide a useful comparison to this research. Other similar research includes the work of Zayas et al.[10]

Andersen et al. investigate the use of deformable trailing edge geometry (DTEG) for load reduction, as part of the ADAPWING project.[8] Rather than using a hinged or rigid flap, a deformable trailing edge

geometry (DTEG) is used. The simulations performed by the authors utilize the HAWC2 aeroelastic code and the NREL/Upwind 5 MW reference turbine as the wind turbine model.[11] Five independent DTEG's are distributed along the blade and pitot tube sensors are used for inflow measurements.

McCoy and Griffin investigate a different type of distributed load control device for smart rotor control, namely microtabs.[9] Microtabs are small translational tabs that deploy orthogonally to either the pressure or suction surface of the airfoil, near the trailing edge, and are capable of altering the lift on the section.[12] The authors simulate the operation a 2.5 MW, 90 m diameter, wind turbine using the ADAMS dynamic simulation software, coupled with Aerodyn subroutines for the aerodynamic calculations. Microtabs, which can deploy with no time lag, are positioned at inboard, midspan, and outboard locations; a more detailed description of the spanwise distribution is not provided.

I.B. Overview of Research

Both experimentally and in simulations, smart rotor control concepts have been demonstrated, and the results indicate that these approaches hold a great deal of promise. This research strives to build upon the success of prior investigations, and to address relatively untreated questions relevant to smart rotor control, by simulating the operation of a 5 MW turbine equipped with trailing edge flaps in an aeroelastic design code, GH Bladed. Specifically, the major questions addressed in this research are:

1. How do trailing edge flaps (TEFs) perform for fatigue load reduction purposes in a turbulent wind field? Essentially, this question aims to evaluate the performance of TEFs for fatigue load reductions, and compare the load reduction capabilities to the baseline controller, individual pitch control, and other smart rotor control investigations.

2. How do these smart rotor control approaches affect the pitch and power systems of the turbine? This question aims to evaluate integration of these devices into an operating wind turbine.

II. Modeling and Procedure

This section describes the modeling procedure and research needed to simulate the operation of a wind turbine equipped with smart rotor control devices, namely trailing edge flaps. The aeroelastic simulation code that is used (GH Bladed), the turbine model used, the controller design methodology, and the simulation details are presented here.

II.A. Turbine Model and Simulation Environment

The simulation of a 5 MW wind turbine with controllable trailing edge flaps is carried out using the aeroelastic simulation package GH Bladed. Some of the important features that Bladed provides are:

- Aerodynamics are calculated using the well-known Blade Element-Momentum (BEM) approach. Dynamic inflow and dynamic stall models are also incorporated to model the turbine wake and deal with unsteady aerodynamic conditions.

- The structural dynamics of the turbine model are calculated using a limited degree of freedom modal model.

- The dynamics of the power train (shaft, gearbox, and generator) are modeled.

- The external wind conditions can be generated, including 3D turbulent wind fields, wind shear, tower shadow effects, and prescribed gusts.

- Control of the turbine can be accomplished using either internal controller provide by Bladed, or external controllers written by the user can be incorporated.

- The loads on the various components of the turbine and the turbine performance are calculated.

II.A.1. NREL/UpWind 5 MW Turbine

The wind turbine model used for the analysis in Bladed is the UpWind 5 MW (also referred to as the NREL 5 MW) wind turbine.[11] This turbine is used as a baseline model for smart rotor control research in the UpWind project. The turbine is a variable speed, pitch controlled turbine, with a 126 m rotor diameter, 90 m hub height, and 20 m water depth.

II.A.2. Trailing Edge Flaps

Bladed is capable of including trailing edge flaps in the turbine model, and allows the TEFs to operate concurrently with variable speed, pitch controlled operation. The TEFs are added to the blade planform from 70% to 90% span. For this section of the blade, the airfoil is a NACA 64618. The TEFs are chosen to have a chordwise length of 10% and a deflection range of ± 10 degrees. These dimensions and deflection ranges are chosen partially based on the work of Troldborg,[13] who investigated the effectiveness of trailing edge flaps for a variety of configurations. Partially, these values are chosen as simply 'reasonable' values, that approximate the configurations of other studies. This research is not an attempt to optimize the configuration of TEFs; rather, it investigates how a given configuration performs during operating wind turbine conditions.

The aerodynamic effects of the TEFs are determined using XFOIL 6.9, which is a 2D viscous panel code developed at MIT.[14] XFOIL is used to generate the coefficients of lift, drag, and pitching moment as a function of angle of attack, for TEF deflection angles ranging from -10 degrees to 10 degrees in 1 degree increments. A Reynolds number of 6 million is used for these calculations. The aerodynamic data generated by XFOIL are then loaded in Bladed as a series of airfoil data sets; one for each TEF deflection angle.

II.B. Turbine Control

External controllers, written in Fortran and compiled as .dll files, are used to control the wind turbine model in Bladed. These external controllers control the generator torque, blade pitch, and TEF deployment angles based on measured signals of the turbine states provided by Bladed.

II.B.1. Standard Control

A baseline controller for the wind turbine model is provided by NREL. This is the "standard controller" for the NREL/UpWind 5 MW turbine model, and so it controls the generator torque and blade pitch, but does not control the TEFs. The generator torque control is a quadratic function of the generator speed in region 2 for optimal tip speed ratio operation. In region 3, the generator torque is used to produce constant power output of the turbine, by setting the demanded torque equal to the rated power divided by the HSS rotational speed. Finally, in region 2.5, the generator torque increases linearly as a function of generator speed, connecting region 2 and region 3. The collective blade pitch is also used to control the turbine speed in region 3. A basic PID controller is used to control the collective blade pitch angle, where the difference between the actual generator speed and the rated generator speed is used as the error signal by the controller. The gains of the PID controller are scheduled so that they decrease as the blade pitch increases.

II.B.2. Load Reduction Controller Design

A more advanced controller than the standard controller is needed to implement a smart rotor control approach and reduce the loads on the rotor blades. Similar challenges are faced when implementing TEFs (henceforth referred to as individual flap control or IFC) or individual pitch control (IPC) schemes, and similar solutions are needed. In fact, the structure of the control approach for IFC and IPC is identical, and the only differences are the gains and the switching logic. Thus, a general "load reduction controller" is described first.

The load reduction controller requires additional control action compared to the standard controller in order to reduce the loads on the blades. In this approach, the standard controller logic remains unchanged, and so the generator torque and the collective blade pitch are controlled in an identical manor, while simultaneously the load control action, either deployment of the TEFs or the individual blade pitch, is performed independently in order to reduce the loads on the blades.

Broadly, the goal of the load reduction control approach is to affect the blade root flapwise bending moment of each of the three blades (M_{y1}, M_{y2}, and M_{y3}), by adjusting either the TEFs or the blade

pitch angles. This is a feedback control approach, and so the TEFs or blade pitch are changed based on measurements of M_{y1}, M_{y2}, and M_{y3}. The major challenge in implementing this feedback control approach is due to the fact that the blades are in a rotating coordinate system, and so the equations of motion that relate M_{y1}, M_{y2}, and M_{y3} and the TEFs or blade pitch contain periodic coefficients. The result is a linear time varying ("LTV") system, and it is much more difficult to implement controllers for LTV systems than linear time invariant (LTI) systems.

The issue of a rotating coordinate system has been identified numerous times in smart rotor control research.[5,6,7,9,15] The most common solution is a multi-blade transformation, or Coleman transformation, which maps the individual blade variables in the rotating frame of reference into a fixed reference frame.[16] In general, while the Coleman transformation is commonly used in practice, there seems to be some confusion regarding the effects of its use. Using this transformation, the blade coordinates are mapped into the fixed nacelle-tower coordinates. For simple turbine models, it appears that all periodic terms are removed from the equations of motion, yielding a completely LTI system,[5].[7] On the other hand, for more complex models of wind turbines, such as the non-linear models used in Bladed, the Coleman transformation has the effect of removing most periodic terms. Bir argues that applying the Coleman transformation does not result in a time-invariant system, but instead acts as a filter which removes all periodic terms except for integral multiples of 3P terms.[15] At the very least, it seems that the 1P periodic terms are removed and so LTI feedback can be used to reduce the 1P loads. In practice, it appears that the approach used in most research is to transform the blade variables into fixed coordinates using the Coleman transformation, and assume an LTI system and implement LTI control techniques such as proportional-integral-derivative (PID) controllers primarily for reducing the 1P loads, while ignoring the remaining periodic components. For this research, it is uniformly assumed that it is appropriate to utilize LTI feedback as described in this section.

The Coleman matrix, P, and its inverse, P^{-1}, for a three bladed wind turbine are shown in Eq. (1) and Eq. (2), respectively, where $\psi(t)$ is the azimuthal angle for each blade, and $\psi(t) = 0$ occurs when a blade is positioned vertically upwards. P^{-1} is used to transform variables in the rotating frame of reference into the fixed frame, and P transforms variables from the fixed frame of reference into the rotating frame. The variables in the fixed and rotating coordinate systems are related according to Eq. (1) and Eq. (2).

$$\begin{bmatrix} \theta_1(t) \\ \theta_2(t) \\ \theta_3(t) \end{bmatrix} = \begin{pmatrix} 1 & \sin\psi_1(t) & \cos\psi_1(t) \\ 1 & \sin\psi_2(t) & \cos\psi_2(t) \\ 1 & \sin\psi_3(t) & \cos\psi_3(t) \end{pmatrix} \begin{bmatrix} \theta_1^{cm}(t) \\ \theta_2^{cm}(t) \\ \theta_3^{cm}(t) \end{bmatrix} \tag{1}$$

$$\begin{bmatrix} M_{y1}^{cm}(t) \\ M_{y2}^{cm}(t) \\ M_{y3}^{cm}(t) \end{bmatrix} = \frac{1}{3} \begin{pmatrix} 1 & 1 & 1 \\ 2\sin\psi_1(t) & 2\sin\psi_2(t) & 2\sin\psi_3(t) \\ 2\cos\psi_1(t) & 2\cos\psi_2(t) & 2\cos\psi_3(t) \end{pmatrix} \begin{bmatrix} M_{y1}(t) \\ M_{y2}(t) \\ M_{y3}(t) \end{bmatrix} \tag{2}$$

θ_1, θ_2, and θ_3 are either the TEF deployment angles or the pitch angles of each blade in rotating coordinates, and a superscript "cm" denotes variables in the fixed coordinate system. The variables in fixed coordinates are defined as follows:

- M_{y1}^{cm} is the average blade root flapwise bending moment, and as such is not a particularly useful variable.
- M_{y2}^{cm} is proportional to the yaw moment exerted by the blades on the fixed hub of the rotor.
- M_{y3}^{cm} is proportional to the tilt moment exerted by the blades on the fixed hub of the rotor.
- θ_{y1}^{cm} is the average, or collective, TEF deployment angle or blade pitch angle.
- θ_{y2}^{cm} is a differential TEF deployment angle or a differential pitch angle in the yaw-wise axis orthogonal to θ_{y3}^{cm}.
- θ_{y3}^{cm} is a differential TEF deployment angle or a differential pitch angle in the tilt-wise axis orthogonal to θ_{y2}^{cm}.

θ_{y2}^{cm} and θ_{y3}^{cm} define how the three individual TEF angles or pitch angles vary from the collective angle. Bossayni has a good description of this process.[1] It has been shown that the variables in the tilt-wise axis and in the yaw-wise axis (Bossayni refers to them as the "d-q axes"[6]), in the fixed coordinate system, are

nearly independent, and so the system can be decoupled into two independent, single input-single output (SISO) systems,[5].[6] Specifically, the differential signal θ_{y2}^{cm} directly controls the yaw-wise bending moment M_{y2}^{cm}, and θ_{y3}^{cm} directly controls the tilt-wise bending moment M_{y3}^{cm}. Bossayni points out that the assumption of independence between variables in the two axes is not entirely correct, but for this investigation the interaction between the axes is ignored for simplicity.[6]

The collective TEF deployment angle or blade pitch angle, θ_{y1}^{cm}, directly control the rotor speed of the turbine (this is not surprising as in the standard control case the collective blade pitch is used to regulate the rotor speed). Thus, this collective loop is not used for load reduction, but instead for rotor speed control. In the case of IPC, the standard controller logic determines the behavior of the collective pitch angle, as if no individual pitch control actions were taking place. In the IFC case, the collective TEF deployment angle is an extra degree of freedom, which may be neglected by setting the value to zero at all times, or it can be used to augment rotor speed control by acting simultaneously with the standard controller collective pitch action. This possibility is discussed in more detail later.

II.B.3. Load Reduction Controller Architecture

By using the multi-blade coordinate transformation, it is assumed that three independent, LTI SISO feedback loops result. LTI SISO systems are easily dealt with from a control perspective, as classical control techniques such as proportional-integral-derivative (PID) control can be employed. Once again, it is important to emphasize that only two feedback loops are needed to control the loads on all three blades. Thus, the control architecture used to reduce the loads on the blades is summarized as follows:

1. The blade root flapwise bending moments of the blades, M_{y1}, M_{y2}, and M_{y3}, are transformed into the fixed frame of reference using P^{-1}, yielding M_{y2}^{cm} and M_{y3}^{cm}, the hub yaw-wise and tilt-wise moments respectively.

2. The transformed loads, M_{y2}^{cm} and M_{y3}^{cm}, are used as inputs to a controller, and the control actions in the fixed frame, θ_{y2}^{cm} and θ_{y3}^{cm}, are calculated. Because the variables are in a fixed frame, this is an LTI system.

3. The control actions in the fixed frame, θ_{y2}^{cm} and θ_{y3}^{cm}, are transformed into the rotating frame using P. These are the demanded control actions of the TEFs or the blade pitch, θ_1, θ_2, and θ_3.

This approach can also be visualized using figure 1.[5] A variety of control approaches are possible using this method of multi-blade transformation. While PID controllers are easily implemented, more complex control approaches such as linear-quadratic-regulator (LQR) techniques can be used, and have been employed in the past.[9,1] The research presented here, however, is not focused on optimal control design. Rather, the goal is to design a "good" controller, that is easily implemented and that achieves sizable load reduction. Thus, PID control techniques are used exclusively, which have been shown to be nearly as effective as more complex LQR techniques anyway.[1] In a PID scheme, the control action, u, as a function of the output signal used for feedback, y, is shown in Eq. (3).

$$u = K_P y + K_D \dot{y} + K_I \int_0^t y dt \tag{3}$$

II.B.4. Controller Implementation

For the IFC case, the deployment range of the TEFs is limited to ± 10 degrees, and the rate of change of the TEF deployment angle is limited to ± 40 degrees per second. Thus, the TEFs may traverse their entire range of deployment in 0.5 seconds. The TEFs are used for load reduction across all operating ranges, including regions 2 and 3.

As discussed previously, in the case of IFC the collective TEF angle is an extra degree of freedom, unused for load reduction. This flexibility can be exploited by using the collective TEF angle to also help control the rotor speed for power regulation in region 3, in order to augment the collective pitch angle that is used for this purpose, and potentially result in smoother power production and less wear on the pitch system. Thus, a simple proportional controller is used to control the collective TEF angle, with the generator speed error used as the input signal to the controller. The collective TEF angle has a position limit of ± 5 degrees, so as

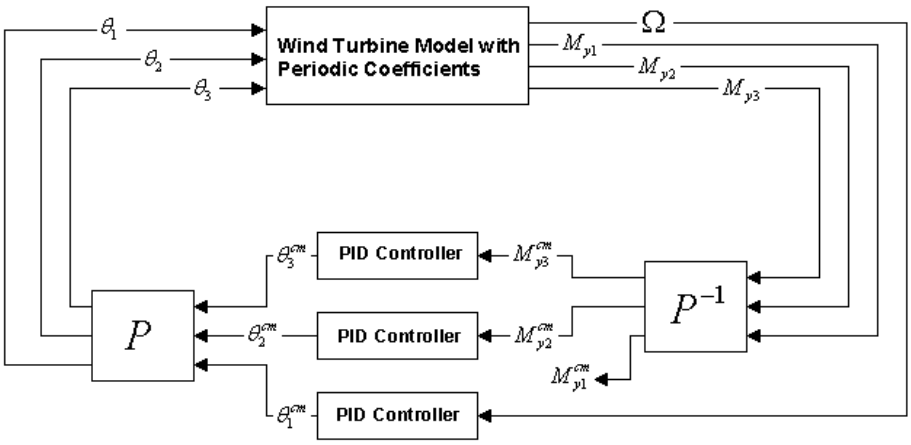

Figure 1. Feedback Control Diagram for Load Reduction Controller

not to drown out the TEF deployment for load reduction. This collective TEF angle is then superimposed on the individual angles used for load control, θ_1, θ_2, and θ_3, and then the position and rate limits are applied to the TEF deployment angle on each blade. There is switching logic required for the collective TEF angle; namely, collective TEF deployment for rotor speed control is only used when the collective pitch angle is greater than 5 degrees.

The IPC controller is implemented in a slightly different manner. First, IPC is only utilized in above rated conditions (region 3), similarly to collective pitch control. The same switching logic used for collective pitch control is applied to IPC. Next, once the individual pitch angles, θ_1, θ_2, and θ_3, are calculated, they are superimposed on the collective pitch angle, and then the position and rate limits of the pitch system are applied to the demanded pitch signal for each blade. The position limits are 0 degrees to 90 degrees, and the rate limit is ± 8 degrees per second.

II.B.5. Controller Gains

The controller gains are determined in an iterative way. For IPC, the gains are chosen at a single operating point, and then the same gain scheduling rule used for the collective pitch command is used for these gains. The IPC gains are determined by simulating the operation of the turbine in turbulent wind with a mean value of 15 m/s. The gains were then adjusted until there was a significant reduction in the standard deviation of the blade root flapwise bending moment, $\sigma(M_{y1})$, without saturating the imposed pitch rate limits. The values of the proportional, integral, and derivative gains are shown in table 1.

Table 1. IPC Gains

Proportional	Integral	Derivative
0.001	0.001	0.0001

These gains are used for both the yaw-axis variables and the tilt axis variables. The units of M_{y2}^{cm} and M_{y3}^{cm} are 10^6 Nm, and the units of θ_{y2}^{cm} and θ_{y3}^{cm} are in radians. The gains are scheduled according to Eq. (4), where θ_{COL} is the collective pitch angle in radians.

$$GS_{IPC} = \frac{1}{1 + 4.55\theta_{COL}} \tag{4}$$

For IFC, the gains are chosen at several operating points. Simulations are performed with turbulent wind inputs at mean wind speeds of 8, 12, 16, and 20 m/s. The gains are adjusted to prevent saturation of the TEF position limits (i.e. to avoid "bang-bang" control action), while still achieving substantial load reduction, measured as the reduction in $\sigma(M_{y1})$. Likewise, the proportional collective flap gain is adjusted so that the collective pitch action is reduced, without saturation of the TEF position limits. The values of

the proportional, integral, and derivative gains for load reduction and the collective TEF proportional gain are shown in table 2.

Table 2. IFC Gains

Proportional	Integral	Derivative	collective
-0.09	-0.03	-0.0015	-0.05

The load reduction gains are used for both the yaw-axis variables and the tilt axis variables. The units of M_{y2}^{cm} and M_{y3}^{cm} are 10^6 Nm, and the units of θ_{y2}^{cm} and θ_{y3}^{cm} are in radians. For the collective TEF controller, the units of the generator speed error is radians per second, and the units of the collective TEF deflection is radians. The gains for the IFC controller are scheduled according to table 3.

Table 3. IFC Gain Scheduling

Wind Speed Range [m/s]	≤ 10	10-14	14-18	18-24	≥ 24
Gain Schedule Value	1	0.5	0.4	0.3	0.2

Again, this research does not aim to develop optimal control approaches to this problem, which is work for future investigations, and because system identification techniques are not utilized, stability of the system cannot be guaranteed. Instead, controllers that are easily implemented and achieve acceptable results are the goal, and the results indicate that this is indeed the case.

II.C. Simulations Run

A variety of simulations are performed in Bladed in order to evaluate the effectiveness of the load reduction controllers, and to investigate the interaction and integration of smart rotor control concepts with the operation of a wind turbine. The external conditions used in the simulations, or load cases, are derived from the International Electrotechnical Commission (IEC) standards, specifically "IEC 61400-1 Ed.3: Wind turbines - Part 1: Design requirements."[17]

To date, two main classes of load cases have been considered: the Normal Turbulence Model (NTM) and the Extreme Turbulence Model (ETM). The site is assumed to be class II_B, with $V_{ref} = 42.5$ m/s, and $I_{ref} = 0.14$. The simulations are performed at mean wind speed values of 8, 12, 16, and 20 m/s, using 3D turbulent wind generated using a von Karman spectrum. The associated logitudinal turbulence intensities for each mean wind speed value, for both the NTM and ETM simulations, are shown in table 4. Also, in all cases a wind shear power law exponent of α=0.2, and a potential flow tower shadow model are used.

Table 4. Turbulence Intensity Values for NTM and ETM Simulations

Mean Wind Speed [m/s]	8	12	16	20
NTM Turbulence Intensity [%]	20.3	17.0	15.4	14.4
ETM Turbulence Intensity [%]	35.0	25.8	21.2	18.4

All simulations are performed for 600 seconds. For the 8 load cases summarized in table 4, simulations are performed using the standard controller (SC), the IFC load reduction controller, and the IPC load reduction controller.

III. Results and Analysis

The results of the simulations are analyzed in terms of the effect of the IFC and IPC control approaches, relative to the baseline SC results, on fatigue loads, power production, and the pitch system.

III.A. Fatigue Load Reduction

The primary purpose of employing the smart rotor control approaches of either spanwise-distributed trailing edge flaps (IFC) or individual pitch control (IPC) is to achieve reductions in the fatigue loads on the blades,

specifically the blade root flapwise bending moment, M_y. The effectiveness of either approach is quantified as the reduction in the 1 Hz damage equivalent load (DEL) of M_y, $DEL(M_y)$. $DEL(M_y)$ is calculated by converting the M_y into a stress value, and then using a rainflow counting method to determine the number of cycles at various amplitudes. A value of 10 is used for the inverse slope of the S-N curve to calculate the values of $DEL(M_y)$.

III.A.1. Normal Turbulence Model Results

The percent reductions in $DEL(M_y)$ using either IFC or IPC and the NTM load cases, compared to the baseline SC case, are shown in table III.A.1.

Table 5. NTM Fatigue Load Reduction Results

	SC	IFC		IPC	
$\overline{U}$ $[m/s]$	$DEL(M_y)$ $[MPa]$	$DEL(M_y)$ $[MPa]$	Change [%]	$DEL(M_y)$ $[MPa]$	Change [%]
8	6.01	5.24	**-12.8%**	-	-
12	6.94	5.98	**-13.8%**	-	-
16	9.15	7.81	**-14.6%**	8.01	**-12.5%**
20	9.90	8.65	**-12.6%**	8.47	**-14.4%**

Table III.A.1 indicates:

- The IFC approach produces sizable reductions in $DEL(M_y)$ for all operating points, with the largest reductions occurring for a mean wind speed on 16 m/s.
- No results are given for the 8 and 12 m/s IPC simulations, as the IPC is only utilized a fraction of the time.
- For the 16 m/s simulations, the IFC approach produces larger load reductions, while for the 20 m/s simulations the IPC approach produces larger load reductions. It should be noted that there are some instances of below rated operation during the 16 m/s simulation, which may negatively bias the IPC results. As such, the 20 m/s simulation is most likely the best basis for comparison, and it indicates that the IPC approach is somewhat more effective at achieving load reductions. The relative performance between the two smart rotor control approaches is discussed in more detail in the following sections.

III.A.2. Extreme Turbulence Model Results

Next, the percent reductions in $DEL(M_y)$ for the ETM load cases are shown in table 6.

Table 6. ETM Fatigue Load Reduction Results

	SC	IFC		IPC	
$\overline{U}$ $[m/s]$	$DEL(M_y)$ $[MPa]$	$DEL(M_y)$ $[MPa]$	Change [%]	$DEL(M_y)$ $[MPa]$	Change [%]
8	8.33	7.86	**-5.6%**	-	-
12	8.79	7.96	**-9.4%**	-	-
16	10.77	9.41	**-12.6%**	10.18	**-5.5%**
20	11.94	10.38	**-13.1%**	10.01	**-16.2%**

Table 6 indicates:

- The IFC approach again produces sizable reductions in $DEL(M_y)$ for all operating points. However, the reductions are generally less for these load cases compared to the NTM load cases.
- No results are given for the 8 and 12 m/s IPC simulations again, as the IPC is only utilized a fraction of the time.

- The performance of the IPC approach during the 16 m/s simulation is substantially worse compared to the NTM case. It is likely that this is a result of the wind speed being below rated for significant portions of the simulation, due to the high turbulence values, and therefore precluding the IPC approach from being utilized.

- Once again, IPC is more effective at 20 m/s, and this is most likely the best basis for comparison between the two approaches, as the turbine operates uniformly in above rated conditions.

Lastly, it should also be noted that reductions in $DEL(M_y)$ for the IFC simulations presented in table III.A.1 and table 6 are negligibly affected by utilizing the collective TEF deployment angle. That is, the load reductions are nearly identical if the proportional gain for the collective TEF deployment is set to 0. Thus, there appears to be no downside to utilizing collective TEF action.

III.B. Time Series Results

It is informative to view the time series of some of the key variables from the simulations, which highlights both the loads that the blade actually experiences, and how the load reduction mechanisms, either TEFs or blade pitch, behave to mitigate these loads. The time series results shown here all come from the NTM simulations with a mean wind speed of 20 m/s. The time series results for simulations at other mean winds speeds and for the ETM cases are similar, except for the IPC simulations at 8 and 12 m/s during which the pitch system is rarely used.

Figure 2 shows a 20 second window of M_{y1} for both the SC and IFC simulation at 20 m/s (NTM), as well as the deflection of the TEF for the first blade.

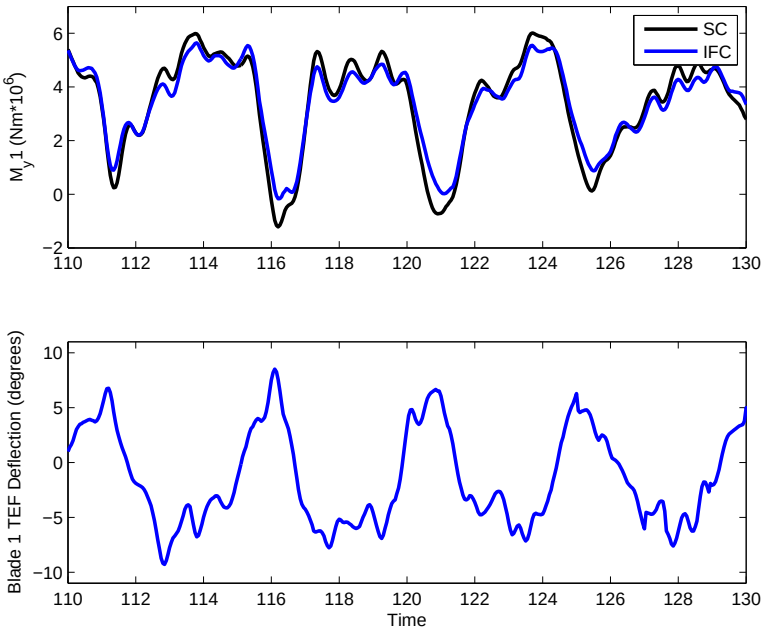

Figure 2. Load Reduction using IFC

Several observations can be drawn from Figure 2:

- There is a strong 1P signal in the the blade root flapwise bending moment, M_{y1}. This is likely due to wind shear, gravity loads, and tower shadow, all of which result in 1P loading.

- In comparing M_{y1} for the SC and IFC cases, it is clear that the TEF behavior reduces the variability in the M_{y1} signal, and this observation is reenforced by the reduction in $DEL(M_y)$ shown in Table III.A.1.

- The TEF behavior shows a strong 1P signal as well, which is 180 degrees out of phase with the M_{y1} signal. This is a logical result, indicating that during periods when the load, M_{y1}, is increasing on the blade, the TEF deflects in a negative fashion in order to reduce the lift on that blade section, and therefore reduce M_{y1}. In general this indicates that the TEFs are behaving appropriately and lends confidence in the implementation of the load reduction controller.

Figure 3 shows the same 20 second window as Figure 2, except the results from the IPC simulation are displayed instead of those from the IFC simulation. Along with M_{y1}, the blade pitch angle for the first blade during this period is also shown.

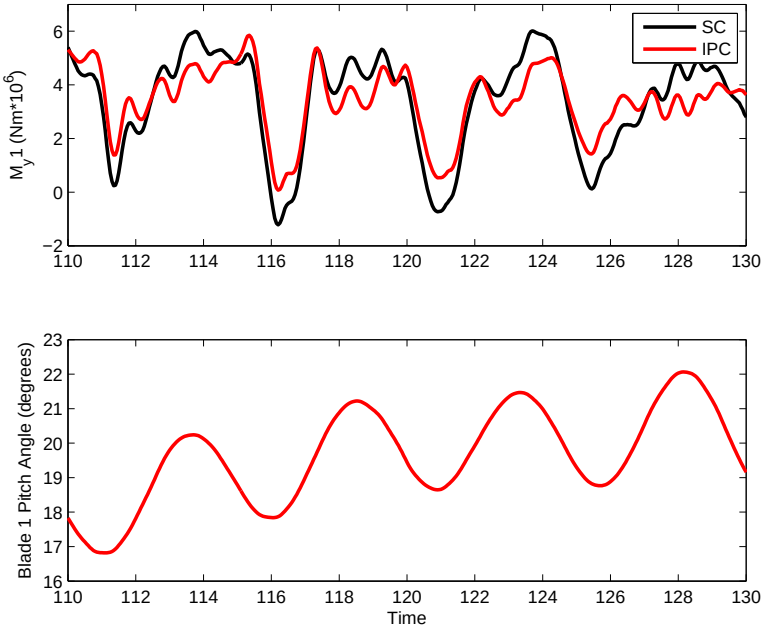

Figure 3. Load Reduction using IPC

Several observations can be made regarding Figure 3:

- As with the IFC simulation, in comparing M_{y1} for the SC and IPC cases, it is clear that the blade pitch behavior reduces the variability in the M_{y1} signal, and this observation is again reenforced by the reduction in $DEL(M_y)$ shown in Table III.A.1.
- The blade pitch behavior shows a strong 1P signal as well, which is in phase with the M_{y1} signal. During periods when the load is increasing on the blade, the blade pitch deflects in a positive fashion in order to reduce the angle of attack, and therefore the lift on that blade, and therefore reduce M_{y1}.

Finally, Figure 4 shows the behavior of all three TEFs during the same 20 second window, and the behavior of all three blade pitch angles. The collective TEF deployment angle and collective pitch angle are also shown in Figure 4. For the IFC case, the collective TEF deployment angle is quite small, whereas for the IPC simulation the collective pitch angle is approximately 19 degrees in order to regulate the speed of the rotor. Clearly, while the collective TEF may help in regulating the speed, the collective pitch system is still the primary means of speed regulation. Both the TEF angles and the pitch angles for each blade are approximately 120 degrees out of phase in Figure 4. It appears that each TEF (or blade pitch) is utilized to primarily reduce 1P loads on the blades.

III.C. Frequency Domain Results

The reduction in fatigue loads using either IFC or IPC can also be analyzed in the frequency domain, by calculating the power spectral density (PSD) of M_{y1} for the SC, IFC, and IPC cases. This also yields insight

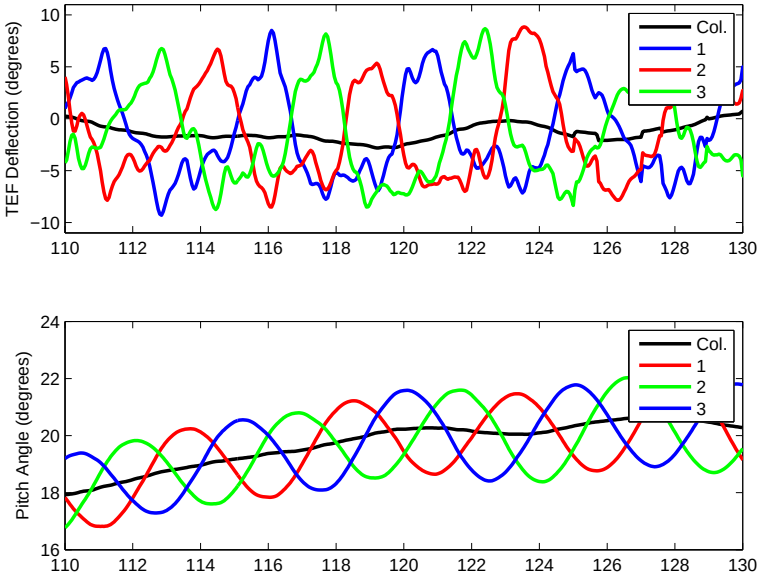

Figure 4. TEF and Blade Pitch Behavior

into the frequency distribution of the loads, and how IFC and IPC perform as a function of the frequency of the loads. Again, the NTM simulations with a mean wind speed of 20 m/s are analyzed exclusively, although for the frequency domain analysis, all 600 seconds of the data set is used to generate the results. The PSD of M_{y1} for the SC, IFC, and IPC cases is shown in Figure 5. The upper and lower plots show the same data, with the upper zoomed in on the peak at 0.2 Hz, and the lower plotted with a logarithmic y-axis.

Figure 5 indicates:

- The PSDs reveal a large 1P peak (∼0.2 Hz) in all cases, which confirms the observations of a 1P signal in the time domain in Figure 2 and Figure 3.
- Both the IFC and IPC approaches result in sizable reductions in the 1P peak of the PSD of M_{y1}.
- The reduction of the 1P peak is larger for the IPC case than the IFC case. This is logical given the larger load reductions noted in the 20 m/s simulation in Table III.A.1.
- For the higher frequency loads, greater than the 1P load at 0.2 Hz, the IFC case results in larger reductions of the PSD compared to the IPC case. In fact the IPC case appears to reduce loads only in the frequency range near the 1P peak.

The dominance of the 1P peak makes it difficult to visually investigate the load reduction capabilities of IFC and IPC at other frequencies even when the logarithmic scale is used. As an alternative, the amount of load reduction as a function of frequency can be determined by integrating the PSDs. The integral of a PSD over a given frequency range is a measure of the energy in the signal within that frequency range. In order to separate the dominant 1P loads from the higher frequency loads, the PSDs were integrated from 0 Hz to 0.25 Hz, which encompasses a "low frequency" region, and from 0.25 Hz to 10 Hz (the Nyquist frequency), which encompasses a "high frequency" region. In this way, the load reduction capabilities of IFC and IPC can be evaluated in terms of their effectiveness at reducing either low frequency or high frequency loads. These results are shown in table III.C.

The results in Table III.C indicate that the IPC approach is more effective than the IFC approach at reducing the low frequency loads. This is readily apparent from Figure 5 as well, as the 1P peak is reduced more using IPC than IFC. The 1P peak is the dominant load source, as 86% of the total energy in the signal is in the low frequency region, and so larger load reduction in the low frequency region when using IPC

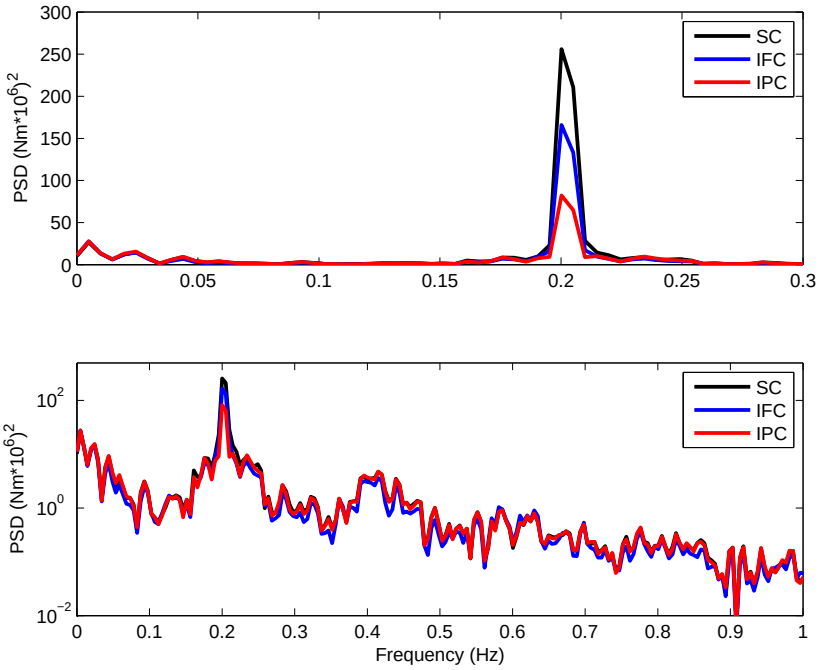

Figure 5. M_{y1} **in the Frequency Domain**

Table 7. Load Reductions in Low and High Frequency Region

Frequency Region	% of Total Energy	Change: IFC [%]	Change: IPC [%]
Low	86%	-29.0%	-47.9%
High	14%	-20.7%	-2.2%

compared to IFC determines the overall larger load reduction when using IPC. On the other hand, in the high frequency region, IFC is significantly more effective than IPC in terms of load reduction. This confirms the observations of Figure 5, which also indicated that IFC was more effective at higher frequencies. While the scale of these loads in much smaller in magnitude compared to the low frequency loads, it nonetheless indicates that IFC is much more capable of affecting high frequency loads. This result should not be surprising, as the TEFs are much smaller than the blades themselves, and so their smaller inertia allows them to react much more rapidly and therefore reduce higher frequency loads. Essentially, these results demonstrate the higher bandwidth of IFC compared to IPC.

III.D. Power Production and Blade Pitch Results

While the principal goal of implementing smart rotor control devices such as TEFs is reducing the fatigue loads on rotor blades, one of the primary objectives of this research is to establish how the integration of these devices affects the operation of a wind turbine. As the TEFs are operating to reduce blade loads, the generator torque and blade pitch are simultaneously controlled for power and speed regulation. Thus, it is important to determine if the TEFs affect these other control objectives, and if so, to identify these potential problems and suggest possible solutions. Furthermore, any opportunities in which TEFs can actually be beneficial to these other control objectives should be determined as well. The effects of using either IFC or IPC on the pitch and power system are presented here, for above rated conditions only. Because the blade pitch is not utilized in below rated conditions, these situations are ignored at present.

III.D.1. Power Production Results

In above rated conditions, the goal is to produce constant (rated) power. In the standard controller case, both the generator torque and the blade pitch are used to achieve this result. In the IFC case, the collective TEF deployment angle is also used to contribute to power regulation. The simulations at a mean wind speed of 20 m/s, for both the NTM and ETM load cases, are most useful for investigating the power production behavior, as there is no switching to below rated conditions in these cases.

Table 8. Above Rated Power Production, 20 m/s Simulations

	SC	IFC		IPC	
Load Case	$\sigma(P)$ $[kW]$	$\sigma(P)$ $[kW]$	Reduction [%]	$\sigma(P)$ $[kW]$	Reduction [%]
NTM	32.1	28.7	**-10.4%**	32.3	**0.9%**
ETM	43.6	38.7	**-11.2%**	43.7	**0.2%**

The important results from the perspective of power production are:

- The values of average power for the SC, IFC, and IPC cases are identical for each 600 second simulation, whether in the NTM or ETM load cases. Thus, the use of IFC or IPC appear to have no effect on energy production above rated.
- Not surprisingly then, the average generator torque is also nearly identical across all the simulations.
- On the other hand, the standard deviation of the power production, $\sigma(P)$ is altered when using IFC or IPC. For IFC, the value of $\sigma(P)$ is reduced, while for IPC, $\sigma(P)$ increases slightly.
- It appears that the use of the collective TEF deployment angle is effective at smoothing out the power production of the wind turbine, by reducing $\sigma(P)$. The reduction in $\sigma(P)$ is approximately the same for the NTM and ETM load cases.
- Conversely, IPC slightly increases $\sigma(P)$.

In general, in above rated conditions, there appears to be no downside in utilizing TEFs for load control, and in fact by also allowing the collective TEF angle to contribute to speed control, the variability in the power production can be reduced by approximately 11% on average.

III.D.2. Pitch System Results

Both the pitch angle, θ, and the rate of change of the pitch angle, $\dot{\theta}$, are considered in this analysis, for the first blade. The variables used to assess the pitch system behavior are the standard deviation of the pitch angle, $\sigma(\theta)$, and the standard deviation of the pitch rate, $\sigma(\dot{\theta})$.

The results from the NTM and ETM simulations at 20 m/s for the standard deviation of the pitch angle, $\sigma(\theta)$, are shown in table 9.

Table 9. NTM and ETM Pitch Angle Results, 20 m/s Simulations

	SC	IFC		IPC	
Load Case	$\sigma(\theta)$ $[deg]$	$\sigma(\theta)$ $[deg]$	Change [%]	$\sigma(\theta)$ $[deg]$	Change [%]
NTM	3.22	3.10	**-3.5%**	3.49	**8.5%**
ETM	3.76	3.63	**-3.4%**	4.01	**6.6%**

Several observations can be made regarding table 9:

- When IFC is used, $\sigma(\theta)$ is reduced compared to the SC case, across all simulations.

- This reduction when IFC is used is due to the use of collective TEF deployment in above rated conditions. The collective TEF angle contributes to regulating the rotor speed, and therefore reduces the variations in the pitch angle.
- Conversely, when IPC is used, $\sigma(\theta)$ increases compared to the SC case, across all simulations.
- Not surprisingly, when the blade pitch angle is also used to help reduce the fatigue loads on the blades during IPC, the pitch system is used more, resulting in larger variability in the pitch angle.

The results from the NTM and ETM simulations for the standard deviation of the pitch rate, $\dot{\theta}$, are shown in table 10.

Table 10. NTM and ETM Pitch Rate Results, 20 m/s Simulations

	SC	IFC		IPC	
Load Case	$\sigma(\dot{\theta})$ $[deg/s]$	$\sigma(\dot{\theta})$ $[deg/s]$	Change [%]	$\sigma(\dot{\theta})$ $[deg/s]$	Change [%]
NTM	0.27	0.24	**-10.5%**	1.21	**354%**
ETM	0.40	0.35	**-11.7%**	1.22	**206%**

Several observations can be made regarding table 9:

- When IFC is used, $\sigma(\dot{\theta})$ is reduced compared to the SC case, across all simulations.
- Again, this reduction when IFC is used is due to the use of collective TEF deployment in above rated conditions. The collective TEF angle contributes to regulating the rotor speed, and therefore reduces the variations in the pitch rate.
- Conversely, when IPC is used, $\sigma(\dot{\theta})$ significantly increases compared to the SC case, across all simulations.
- Not surprisingly, when the blade pitch angle is also used to help reduce the loads on the blades, the pitch system is used more, resulting in larger variability in the pitch rate.

III.E. Limitations of Results and Analysis

The results derived from the Bladed simulations provide several useful insights and conclusions regarding the integration and performance of TEFs for load reduction purposes. However, the Bladed simulations rely on a number of assumptions, and it is important to justify some of these assumptions to help establish the validity of the results. In particular, two critical aerodynamic assumptions are made in the simulations that must be assessed: the assumption of steady aerodynamics, and not employing a dynamic stall model. These issues are interrelated but are treated separately here.

III.E.1. Evaluation of Unsteadiness

During the simulations, Bladed assumes quasi-steady aerodynamic behavior of the airfoil sections. That is, during operation as the angle of attack of an airfoil section changes and as the TEF deflects to control loads, the aerodynamic performance of the airfoil, characterized by C_L, C_D, and C_M, is determined directly from the airfoil tables that are input into Bladed. Thus, the aerodynamic performance is calculated in a quasi-steady manner, by assuming that C_L, C_D, and C_M change with each time step dependent solely on the values of α and the TEF deployment angle, and not on how quickly these parameters are changing.

In reality, the aerodynamic performance of the airfoil sections change in a dynamic sense. A rapid change in the angle of attack does not result in an instantaneous change in C_L, C_D, and C_M; instead, C_L, C_D, and C_M change over some period of time until they reach a steady state value. Only when the angle of attack and the TEF deployment angle are changing slowly enough is the assumption of quasi-steady aerodynamics a valid approximation.

When an airfoil section experiences some disturbance, the degree of unsteadiness caused by that disturbance can be quantified by the reduced frequency, k. k is a non-dimensional parameter, and is determined

using Eq. (5), where c is the local chord length of the section, U is the local relative velocity at the section, and ω is the frequency of the disturbance, in units of radians per second.[18]

$$k = \frac{c}{2U}\omega \tag{5}$$

The larger the value of k, the more the actual performance of the airfoil deviates from the performance when one assumes quasi-steady behavior. For example, consider a situation in which an airfoil section is pitched in a sinusoidal manner, changing the angle of attack. For a low frequency oscillation, and so a small value of k, the difference between the actual aerodynamic performance and the performance under the assumption of quasi-steadiness is negligible. But as the oscillation frequency increases, and so k increases, the deviation between the actual performance and the performance under the assumption of quasi-steadiness becomes larger. As a general rule, when $k < 0.05$ the aerodynamics can be considered quasi-steady, and when $k > 0.05$ they are considered unsteady.

An analysis is performed using the simulation results to assess the degree of unsteadiness on the TEF sections. Because the TEFs are rapidly changing in position in order to respond to changes in the loads, it is possible that the aerodynamics are unsteady on these sections. However, the situation is complicated by the fact that the disturbances on the airfoil section are not at one specific frequency, but occur over a range of frequencies. Likewise, the TEFs do not change position at a single frequency. Thus, there is no single specific value for ω in Eq. (5). This problem is solved as follows. The power spectral density (PSD) of the TEF angle, for the first blade at blade station $r = 52.75\ m$, is calculated for each IFC simulation (8, 12, 16, and 20 m/s for NTM and ETM load cases). The result is the PSD as a function of frequency. Next, this frequency vector, originally in units of Hz, is converted to radians per second. Finally, using the local chord at that blade station, $c = 2.518\ m$, and the average local relative velocity over each simulation, the frequency vector is converted to reduced frequency using Eq. (5). The result is the PSD of the TEF deflection angle as a function of reduced frequency, i.e. the spectrum of the unsteadiness. These spectra are shown in figure 6.

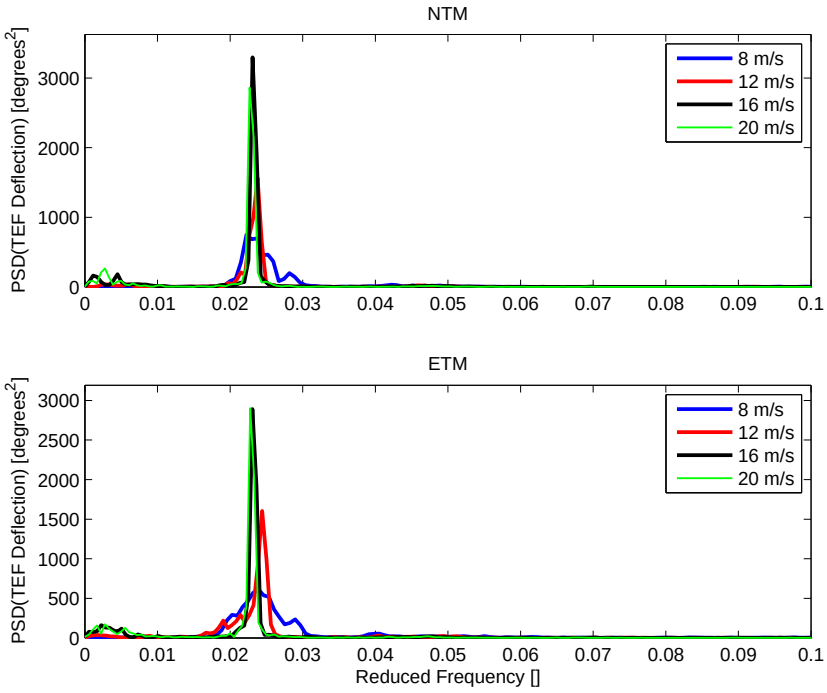

Figure 6. Trailing Edge Flap Deflection Spectrum

Clearly, some of the energy in the TEF deflection signal is in the quasi-steady region, and some is in the unsteady region. Figure 6 can therefore be used to determine how unsteady the behavior of the TEFs actually is. It is clear that the majority of the energy is in the quasi-steady region, as the major peaks in the spectrum occur at a reduced frequency of approximately $k = 0.023$ for all simulations, which is less than the

boundary at $k = 0.05$. Simply by inspection, it therefore appears that the TEF deflection can be treated as a quasi-steady problem. Furthermore, the spectrum of the angle of attack at this section is nearly identical, further reenforcing the steady nature of the behavior.

The degree of unsteadiness can be further quantified by integrating the PSD of the TEF deflection angle between $k = 0$ and $k = 0.05$, and then between $k = 0.05$ and $k = 1.5$ (the maximum value). In this way, the proportion of energy in the quasi-steady and the unsteady regions can be compared. These results are given in table III.E.1, which shows the percentage of energy in the quasi-steady region for each of the simulations. In general, a significant majority of the energy is indeed in the quasi-steady region, approximately 90% or more. This further confirms the steady nature of the aerodynamics on the TEF section. The proportion of energy in the quasi-steady region for the angle of attack spectra is nearly identical to the values in table III.E.1.

Table 11. Proportion of TEF Spectrum in the Steady Region

Mean Wind Speed, m/s	NTM, Steady Proportion, %	ETM, Steady Proportion, %
8	93.9%	89.6%
12	95.4%	94.3%
16	96.6%	96.0%
20	97.2%	96.5%

In sum, while the aerodynamics on the TEF sections are not entirely quasi-steady, it nonetheless appears to be a safe assumption, as the majority of the energy of the PSD for the TEF deployment and the angle of attack is in the quasi-steady region. Finally it should be noted that the degree of unsteadiness depends strongly on the spanwise blade section under consideration. The inboard sections, where the chord length is larger and the relative wind speed is smaller, have larger reduced frequencies. However, there are no TEFs on these sections, and so any errors due to unsteady aerodynamic effects will be constant across all the simulations.It is only on the TEF section where the simulations may differ in terms of unsteady aerodynamic behavior.

III.E.2. Evaluation of Dynamic Stall

In order to include TEFs in the Bladed simulation, the dynamic stall model that is normally employed must be disabled. Dynamic stall models are used to model the aerodynamic performance of an airfoil at angles of attack outside of the static attached flow region (static stall angle). A simple way to evaluate the validity of the assumption of no dynamic stall is by investigating the angle of attack behavior of a blade section during the simulations. If α rarely or never exceeds the static stall angle, then disabling the dynamic stall model results if negligible errors. The static stall angles for the NACA 64618 airfoil are approximately ± 9 degrees.

To investigate this issue, the angle of attack time series from the $r = 52.75$ blade station are compiled for the 8, 12, 16, and 20 m/s simulations using IFC, and for the NTM and ETM load cases. Then a histogram of α values is calculated. The results are shown in figure 7, which shows the histogram of all angle of attack values for the NTM and ETM load cases.

Figure 7 indicates that α never exceeds the static attached flow region, and so the airfoil at this blade station is never stalled. This is an encouraging result, and lends confidence to the results as it demonstrates that a dynamic stall model is evidently not needed for these simulations.

This supposition is further confirmed by comparing the simulation results for the SC and IPC case with and without the dynamic stall model enabled. For the relevant variables, including standard deviation of the blade root flapwise bending moment, average and standard deviation of the power output, average and standard deviation of the pitch angle, and average and standard deviation of the generator torque, the values from the simulations with and without the dynamic stall model enabled are nearly identical. In general, it appears that for the simulations performed in this research, disabling the dynamic stall model does not result in significant error.

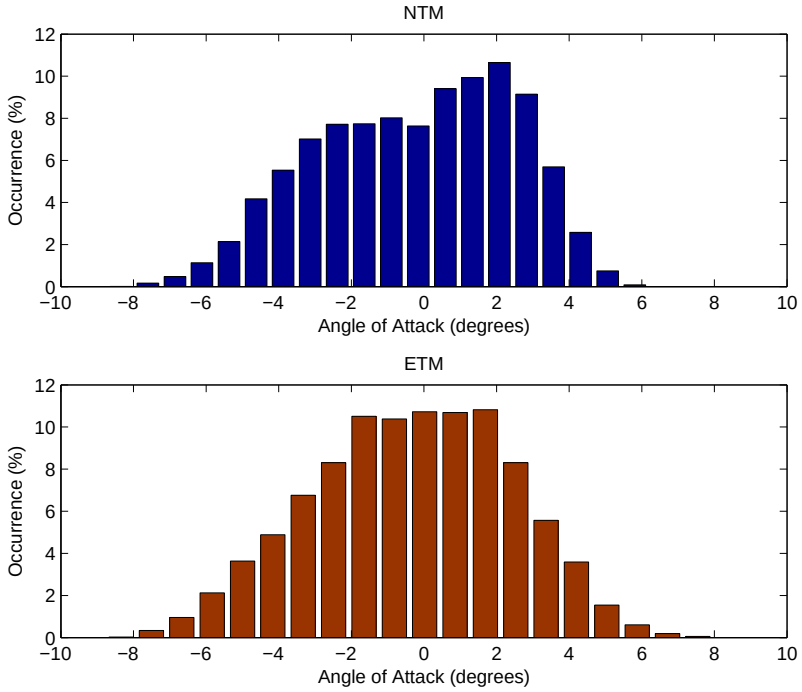

Figure 7. Angle of Attack Histogram

III.E.3. Summary of Limitation Analysis

The preceding analysis indicates that the assumption of quasi-steady aerodynamic behavior, and the lack of a dynamic stall model, are relatively safe modeling assumptions. The results demonstrate that the TEF behavior is predominantly a quasi-steady phenomena, with low reduced frequencies, and that the angle of attack is in the static attached flow region across all operating points. Thus, the modeling assumptions appear to be valid, and this analysis helps to lend credibility to the results of the simulations.

IV. Conclusions

This research strives to both demonstrate the effectiveness of trailing edge flaps for load reductions purposes, compare the performance to another promising load reduction approach, and to investigate the integration of these devices into an operating wind turbine. Ultimately, the goal is not to determine an optimal load reduction approach; rather, the purpose of the research is to address the broader issues of integrating smart rotor control devices into a wind turbine, by identifying both the potential and opportunities for these devices as well as the potential drawbacks and limitations. The major conclusions of this research are:

- Trailing edge flaps can be modeled in GH Bladed and utilized for load reduction investigations. Bladed allows for the aerodynamic properties of the TEFs to be input, and external controllers can be used to implement feedback control methods for load reduction. These methods can also be used to implement individual pitch control algorithms. In sum, Bladed provides a useful platform for testing smart rotor control approaches.

- A number of load cases are simulated using the baseline standard controller, an individual flap controller, and an individual pitch controller. The effectiveness of the two smart rotor control approaches are evaluated based on their reduction of the 1 Hz damage equivalent load of the blade root flapwise bending moment compared to the values obtained using the standard controller. Both methods are capable of achieving sizable load reductions, and the relative performance depends on the specific

load case. While IPC more substantially reduces the 1P load signal, the IFC approach appears to be more effective at reducing high frequency loads. These two approaches are analyzed in the time and frequency domain to help highlight their behavior.

- The effect of IFC and IPC on the power output and pitch system of the turbine is also evaluated. In above rated conditions, the IFC approach is able to reduce pitch usage and the fluctuations in the power output by utilizing collective TEF deployment, while the IPC approach results in significantly increased pitch usage and slightly larger power output variability.

- While the assumption of quasi-steady flow and the disabling of the dynamic stall model could lead to errors in the simulations, an investigation into the consequences of these limitations indicates that they are likely to result in negligible errors in the final results.

Acknowledgments

The authors would like to acknowledge STW for funding this research, and Ervin Bossayni, Thanasis Barlas, and Jan-Willem van Wingerden for their contributions.

References

[1]Bossayni, E., "Developments in Individual Pitch Control," *EWEA Special Topic Conference: The Science of Making Torque from Wind*, 2004.

[2]Bossayni, E., *GH Bladed Version 3.80 Theory Manual*, Garrad Hassan and Partners.

[3]Barlas, T., "Smart Rotor Blades and Rotor Control for Wind Turbines: State of the Art," Knowledge base report for upwind wp 1b3, Delft University Wind Energy Research Institute (DUWIND), 2006.

[4]Barlas, T. and van Kuik, G., "State of the art and prospectives of smart rotor control for wind turbines," *The Science of Making Torque from Wind, Journal of Physics: Conference Series*, 2007.

[5]van Engelen, T. and van def Hooft, E., "Individual Pitch Control Inventory," Tech. rep., Technical University of Delft, 2005.

[6]Bossayni, E., "Individual Blade Pitch Control for Load Reduction," *Wind Energy*, Vol. 6, 2003.

[7]Selvam, K., *Individual Pitch Control for Large Scale Wind Turbine*, Master's thesis, Technical University of Delft, 2007.

[8]Andersen, P., Henriksen, L., Gaunaa, M., Bak, C., and Buhl, T., "Integrating Deformable Trailing Edge Geometry in Modern Mega-Watt Wind Turbine Controllers," *2008 European Wind Energy Conference and Exhibition*, 2008.

[9]McCoy, T. and Griffin, D., "Active Control of Rotor Aerodynamics and Geometry: Statues, Methods, and Preliminary Results," *44th AIAA Aerospace Science Meeting and Exhibit*, 2006.

[10]Zayas, J., van Dam, C., Chow, R., Baker, J., and Mayda, E., "Active Aerodynamics Load Control for Wind Turbine Blades," *European Wind Energy Conference*, 2006.

[11]Jonkman, J., Butterfield, S., Musial, W., and Scott, G., "Definition of a 5-MW Reference Wind Turbine for Offshore System Development," TP 500-38060, National Renewable Energy Laboratory, 2008.

[12]Mayda, E., van Dam, C., and Nakafuji, D., "Computational Investigation of Finite Width Microtabs for Aerodynamic Load Control," *43rd AIAA Aerospace Science Meeting and Exhibit*, 2005.

[13]Troldborg, N., "Computational study of the RisøB1-18 airfoil with a hinged flap providing variable trailing edge geometry," *Wind Engineering*, Vol. 29, No. 2, 2005, pp. 89–113.

[14]Drela, M. and Youngren, H., *XFOIL 6.9 User Primer*, MIT.

[15]Bir, G., "Multi-Blade Coordinate Transformation and Its Application to Wind Turbine Analysis," *46th AIAA Aerospace Science Meeting and Exhibit*, 2008.

[16]Coleman, R. and Feingold, A., "Theory of Self-Excited Mechanical Oscillations of Helicopter Rotors with Hinged Blades," Tech. rep., NASA, 1958.

[17]*IEC 61400-1 Ed.3: Wind turbines - Part 1: Design requirements*.

[18]Leishman, J.